Heliyon 7 (2021) e07649

Contents lists available at ScienceDirect

Heliyon

journal homepage: www.cell.com/heliyon

Research article

Bispecific antibodies: A guide to model informed drug discovery and development

Irina Kareva [a,*], Anup Zutshi [a], Pawan Gupta [b], Senthil Kabilan [a]

[a] EMD Serono, Merck KGaA, Billerica, MA, USA
[b] University of Maryland, Baltimore, MD, USA

ARTICLE INFO

Keywords:
Lead compound optimization
Bispecific antibody
KD
Target engagement
Antagonist
Model informed drug discovery and development
Affinity maturation

ABSTRACT

Affinity (KD) optimization of monoclonal antibodies is one of the factors that impacts the stoichiometric binding and the corresponding efficacy of a drug. This impacts the dose and the dosing regimen, making the optimum KD a critical component of drug discovery and development. Its importance is further enhanced for bispecific antibodies, where affinity of the drug needs to be optimized with respect to two targets. Mathematical modeling can have critical impact on lead compound optimization. Here we build on previous work of using mathematical models to facilitate lead compound selection, expanding analysis from two membrane bound targets to soluble targets as well. Our analysis reveals the importance of three factors for lead compound optimization: drug affinity to both targets, target turnover rates, and target distribution throughout the body. We describe a method that leverages this information to help make early stage decisions on whether to optimize affinity, and if so, which arm of the bispecific should be optimized. We apply the proposed approach to a variety of scenarios and illustrate the ability to make improved decisions in each case. We integrate results to develop a bispecific antibody KD optimization guide that can be used to improve resource allocation for lead compound selection, accelerating advancement of better compounds. We conclude with a discussion of possible ways to assess the necessary levels of target engagement for affecting disease as part of an integrative approach for model-informed drug discovery and development.

1. Introduction

Selection and optimization of a lead molecule is one of the most critical steps in early drug development, which can determine much of the success of the compound in the long term, as well as affect the amount of resources that will be required for its development. Therefore, finding scientifically sound theoretical approaches to improve this process can have a profound impact on drug development. While these approaches are applicable for both large and small molecules, our focus here is primarily on biologics.

The mechanism of action of currently developed biologics, like most other drugs, begins with target engagement, with the assumption that blocking or stimulating a particular target can interfere with or promote the signaling cascade that drives pathogenesis. Examples of such molecules include checkpoint inhibitors and T-cell engagers in immuno-oncology [1, 2, 3], anti-inflammatory drugs for autoimmune diseases [4, 5, 6, 7], anti-angiogenesis drugs [8], among others. In the cases when clear understanding of the impact of target engagement is limited due to incomplete knowledge of the downstream biology, one aims to achieve maximal target engagement (typically over 90 %), assuming that at this level any potential effects on downstream signaling will be achieved.

Bispecific antibodies (BsAbs) are designed to bind two targets simultaneously, presumably thereby augmenting the impact on each of the targeted pathways; targets are often assumed to be expressed in the same Site of Action (SoA), although this assumption is not mandatory for a bispecific modality. An advantage of a bispecific is the ability to co-localize the effect of target blockade to a single space, potentially creating an additive or a synergistic effect. A challenge of this approach, however, lies in ensuring sufficiently high levels of target engagement for both targets, which may be affected by different levels of target expression, targets being expressed on different tissues, ubiquitous distribution of one target but a localized distribution of the second target, avidity effects or steric hindrance in the simultaneous binding of the two targets. Each of these factors taken individually or in combination might complicate the disposition and kinetic behavior of the bispecific molecule.

* Corresponding author.
E-mail address: Irina.Kareva@emdserono.com (I. Kareva).

https://doi.org/10.1016/j.heliyon.2021.e07649
Received 11 February 2021; Received in revised form 2 July 2021; Accepted 20 July 2021

Given the importance of maximizing target engagement in the SoA, several models have been developed to assist with lead molecule selection for both mono-specific [9] and bispecific antibodies [10, 11]. One of the key aspects that can be controlled in the drug design and optimization stage is the affinity (KD), i.e., the tightness of binding between the drug and its target. KD is calculated as a ratio between rate of target release k_{off} and the rate of binding k_{on}; numerically smaller values of KD indicate tighter binding between the drug and its target. The process of selecting the molecule with appropriate affinity is referred to as affinity maturation.

Monoclonal antibodies generally act by interfering with native signaling between a target and its native ligand. Optimal KD for a drug is determined not only by the properties of the drug but also by those of its target. Targets for monoclonal antibodies can typically be membrane-bound and expressed on the cell surface (e.g., PD-1), or soluble and expressed in the interstitial space and plasma (e.g., PD-L1). Membrane targets can also shed into a soluble form that can also bind the drug. Targets can be characterized by their expression and turnover levels. Membrane targets that shed, where the latter is an undesirable entity, can bind the drug and affect the eventual dose needed to achieve desired pharmacology (sink effect). Therefore, to determine optimal KD it is necessary to determine binding affinity of the drug to the soluble form of the receptor, as well as membrane bound form, including the binding to membrane bound target in its shed form.

In Tiwari et al. [9], the authors formalized the relationship between KD and target properties for mono-specific monoclonal antibodies based on maximizing predicted target engagement for either soluble, membrane-bound and membrane shed targets. In [11], we extended this work to develop a general model for KD optimization for a BsAb with two membrane-bound targets. The model highlighted the existence of "sweet spots" for membrane-bound targets with high turnover, demonstrating that tighter binding does not necessarily lead to highest target engagement or lowest dose. If the target turnover is very high, then tighter-binding drug will be cleared at a higher rate; instead, a lower KD may be optimal to ensure both high target coverage and lowest possible dose (Figure 1).

Here we extend our previous work in two ways. Firstly, we modify the model introduced in [11] to describe the interactions of a bispecific antibody with one soluble and one membrane-bound target to evaluate whether and how the soluble nature of one of the targets impacts KD optimization. Secondly, we extend our analysis to KD optimization for lower target occupancy thresholds.

The strategy for maximizing target engagement is an excellent approach for achieving a proof of pharmacology. However, striving to achieve over 90 % engagement is not always necessary and may lead to estimation of doses that are higher than needed to achieve a therapeutic effect. Furthermore, the 90 % + target occupancy level is typically applicable for antagonists, or for drugs with good safety profiles. For agonists (CAR-T or Bispecific T-cell engagers), or drugs with narrow safety margins, lower target engagement may be adequate [12, 13]. Finally, in some cases it may not be possible to engage both arms of the bispecific drug at sufficiently high levels due to physiological restrictions in the distribution or turnover of the target(s).

To explore these scenarios, we developed a bispecific antibody KD optimization guide. Here we show how mathematical modeling can help decide whether KD of a bispecific antibody needs to be optimized at all, and if so, which arm and to what extent. We show application of the method to several case studies, where conditions were chosen to illustrate all possible scenarios. We discuss what physiological properties may be particularly important in different scenarios, providing a more general guideline. We conclude with a discussion of applicability and limitations of this approach for model informed drug discovery and development.

2. Methods

This section provides an overview of the proposed approach for KD optimization in bispecific antibodies. We define optimal KD as the one that allows reaching desired target occupancy (TO) with the lowest dose. To achieve this goal, we need to model two aspects of drug-target interaction: pharmacokinetics (PK) and pharmacobinding (PB).

Pharmacokinetic (PK) models describe change in drug concentration over time as the drug travels through the body; here we assume that the drug is administered into the plasma compartment and can distribute into the target tissue, also referred to here as the site of action, and into the peripheral compartment. SoA is the physiological space in which the target(s) responsible for pharmacological signaling are present, while the peripheral compartment is the rest of the tissues in the body, into which the drug can distribute but where no pharmacological effect occurs.

Pharmacobinding (PB) refers to interactions of the drug with its targets. A bispecific antibody by definition can interact with two targets. Here we assume that one of the targets is soluble (S target), and one is membrane-bound (M target). Examples of soluble targets include TNF-alpha, VEGF, and PD-L1; examples of membrane-bound targets include HER-2, VEGF-R, and PD-1. A model with two membrane-bound targets was studied in detail in [11].

We assume that interactions between a drug and both of its targets occur in the SoA, where the latter are intrinsically expressed (synthesized and degraded). Additionally, we assume that the soluble target can be present in the plasma, where it has the same turnover as in the SoA, and can bind to the drug, thereby acting as a drug sink. The detailed model description and corresponding parameter values used in these simulations are given in Appendix. A diagram of the model is shown in Figure 2.

TO is calculated as a ratio of target bound to the drug to the sum of bound and free targets. Our goal is to find KD such that we reach desired TO on both arms of the molecule with lowest possible dose (some considerations about criteria for selecting a desired TO depending on target properties are provided in the Discussion). To do so, we employ the approach we developed in [11] for finding optimal KD for a bispecific

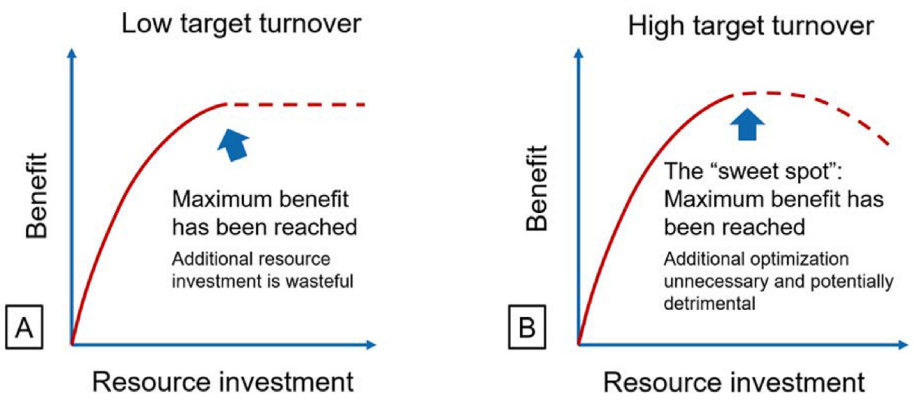

Figure 1. Law of diminishing returns in resource allocation for affinity maturation in compound development. (A) For targets with low target turnover rate, there exists a "good enough" point, beyond which additional resource investment in affinity maturation will not significantly lower the anticipated dose. (B) For targets with high turnover rate, there exists a KD "sweet spot" that allows achieving desired target engagement with lowest dose; further increasing affinity would lead to higher drug clearance and higher dose.

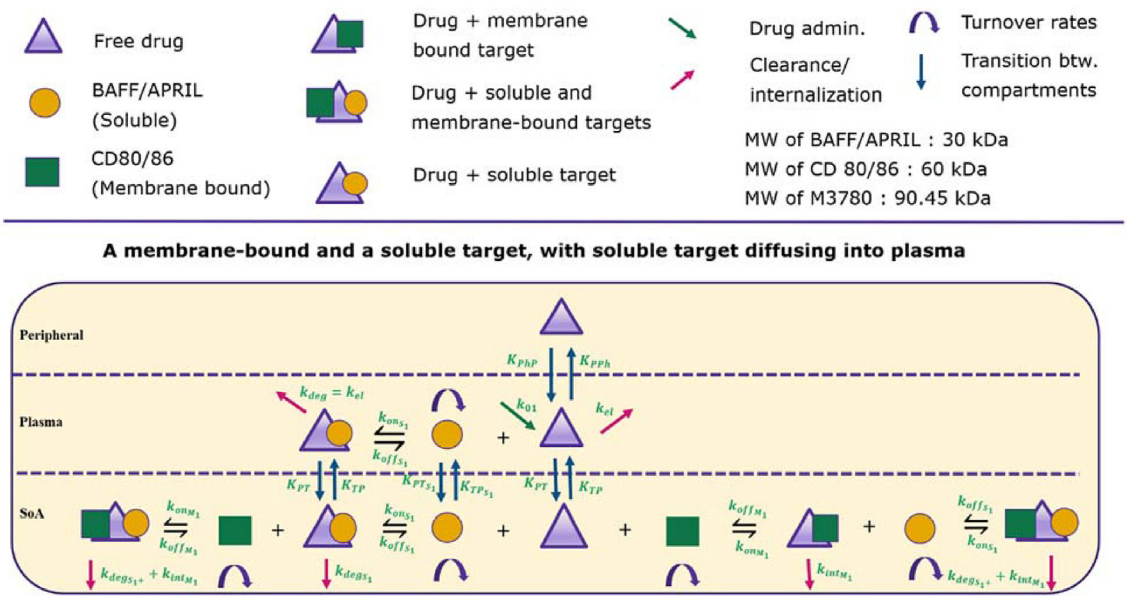

Figure 2. Diagram of a BsAb interacting with a membrane-bound and a soluble target, with interactions between BsAb and membrane-bound target occurring only at the SoA, while interactions with the soluble target can occur both in SoA and in the plasma compartments. It is also assumed that the soluble target is synthesized both in SoA and in plasma, and can diffuse between the two compartments, as can the drug-soluble target complex. The equations describing the dynamics of this case are given in Appendix.

antibody with two membrane-bound targets. We create a sample space of possible physiologically reasonable KD values, run simulations and record the dose at which desired TO was reached for each KD; we then select the KD that corresponds to the lowest dose.

This approach is most effective when all relevant physiological conditions are known, i.e., when the concentrations of both targets are known in the relevant physiological compartments (in this case, SoA for both targets and plasma for S target). However, measuring these values may be resource-intensive, or even unfeasible. To address this challenge, we propose a method that allows performing scenario analysis through sampling a wider set of conditions that may describe the physiological space. This will help to determine whether KD needs to be optimized at all and if so, which arm and under what conditions.

The approach can be applied to both agonists and antagonists. For the former, typically only the membrane-bound arm is of relevance, since signal amplification that can accompany excessive target engagement occurs only for membrane-bound targets [14]. Therefore, for an agonist, an optimal KD would typically correspond to a situation when M arm reaches desired level of target engagement.

For an antagonist, we can seek to guarantee a pre-specific minimum level of target engagement on both arms of the molecule. For the purposes of method illustration, we assume here that the same level of target engagement needs to be reached for both targets; this assumption can be relaxed and modified for specific cases. In what follows, we focus primarily on antagonists that may require lower levels of target engagement for sufficient efficacy, but the analysis can be applied to higher levels of target engagement as well.

2.1. Model inputs

Since the proposed approach is intended to assist in lead compound selection before specific PK properties are identified, we use PK parameter values that are generic but fall within physiological ranges for most monoclonal/bispecific antibodies (see table with parameter values in Appendix). At this stage target properties therefore become key in enabling us to find optimal KD. These include target turnover rates, target concentrations both at the SoA and in the plasma, as well as S target transport rate between tissue and plasma. A summary of relevant inputs

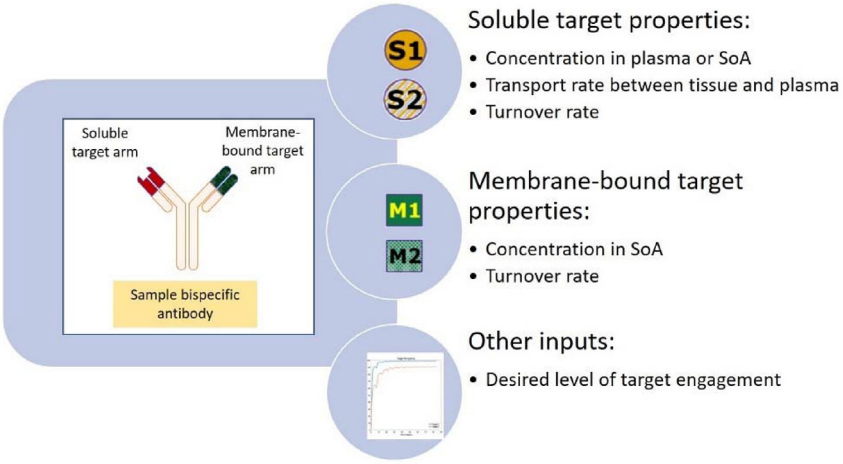

Figure 3. Summary of necessary inputs, which include target properties and desired level of target engagement.

can be found in Figure 3. Notably, it is not critical to have exact values of these parameters in order to apply the proposed approach; instead, we can assume some general set of physiological conditions, and if the simulations reveal the need to optimize KD under a subset of those, we can conduct experiments to help identify more exact physiological values. An example of such scenario will be demonstrated in Case 3. Notably, here we are not including the analysis of target turnover rates, which was done in [11]; conclusions reached in [11] apply for analysis conducted here as well.

With this information, we can now implement the process, described in Figure 4.

Model inputs are the PK model specific to the drug (Figure 2) and anticipated target properties, such as target concentrations in SoA and plasma, target turnover rates, etc (Figure 3). For all the cases described below, we determine optimal KD for weekly dosing of the simulated compound. However, the steps outlined here can be used for any dosing schedule.

2.2. Process overview

For the purposes of introducing the method, we assume that the concentration of M target is known, and concentration of S target is known (perhaps) only in one of the compartments. If the concentration of S target in any of the compartments is known, we can analyze scenarios based on different ratios of S target concentrations in tissue vs plasma, a metric we refer to sTPR (soluble target tissue to plasma ratio).

For various values of sTPR we calculate the dose necessary to achieve desired TO for extreme values of KD for both arms, as well as for a range of sTPR values in between. Here we chose KD = 0.01 nM as a low end and KD = 500 nM as the high end to capture a sufficiently broad range of possible KDs; the range can be expanded or reduced as needed for a specific project. We define Dose 1 as the dose necessary to achieve desired KD when both targets have KD = 0.01 nM; Dose 2 is the dose necessary to achieve desired KD when both targets have KD = 500 nM. We then calculate the difference between Dose 2 and Dose 1, using it for the first decision-making step.

If there is no difference between the doses predicted at both extremes, then KD optimization is unnecessary, and other criteria should be used for lead compound selection. If the difference is positive, i.e., Dose 2 > Dose 1, then the dose is larger when KD is higher (the most typical scenario), and therefore lower KD is going to be optimal. If the difference is negative, i.e., Dose 2 < Dose 1, then the dose is larger when KD is smaller, and weaker binding will in fact allow reaching desired TO with a lower dose. The latter is more likely to occur with targets that have high turnover, as discussed in [9, 11].

An important note should be made about decision-making at Step 1. In a vast majority of cases, the largest dose differential is obtained at KD extremes as specified in Figure 5 (dose when both targets have high KD or dose when both targets have low KD). However, if the analysis reveals that the difference between two maximum doses is below some decision threshold (specific criteria for determining such a threshold will be discussed below), we recommend sampling the intermediate KD space to evaluate whether a larger or smaller dose could be possible. This extra step will allow to increase confidence in the decision of Step 1.

If at Step 1 we identified that KD does need to be optimized, we can then determine which arm of the molecule needs to be prioritized. At Step 2, we run simulations for different levels of sTPR, obtaining a dose and corresponding levels of target engagement on each arm. The decision is then made as follows: for an antagonist, we select the arm that is last to reach desired TO; this is the "limiting" arm that needs to be optimized. For an agonist, we typically optimize the M arm of the molecule, since only the engagement of the M arm and not the S arm can lead to overstimulation. The specific steps necessary to enable decision making at each stage are summarized in Figure 5.

2.3. Decision thresholds

Different criteria can be used to make the ultimate decision about whether the KD needs to be optimized. The simplest criterion is proposed in Step 1 of Figure 5, i.e., calculating whether there exists any difference in predicted dose for different KD values. However, this approach does not provide information on the magnitude of said difference, and therefore there may exist additional criteria that one may consider for making the decision on whether KD needs to be optimized at this step.

Decision thresholds can be determined by a variety of factors that determine the tradeoffs of obtaining a potentially marginal improvement in dose vs financial or temporal investments. While for antagonists these may be the primary considerations, for agonists, where marginal increase in receptor engagement can lead to unacceptable level of risk for the patient (e.g., a cytokine storm), the "zero dose differential" criterion may be the most acceptable one. For these cases, Step 2 becomes particularly critical in ensuring that no more than the acceptable level of target engagement is achieved.

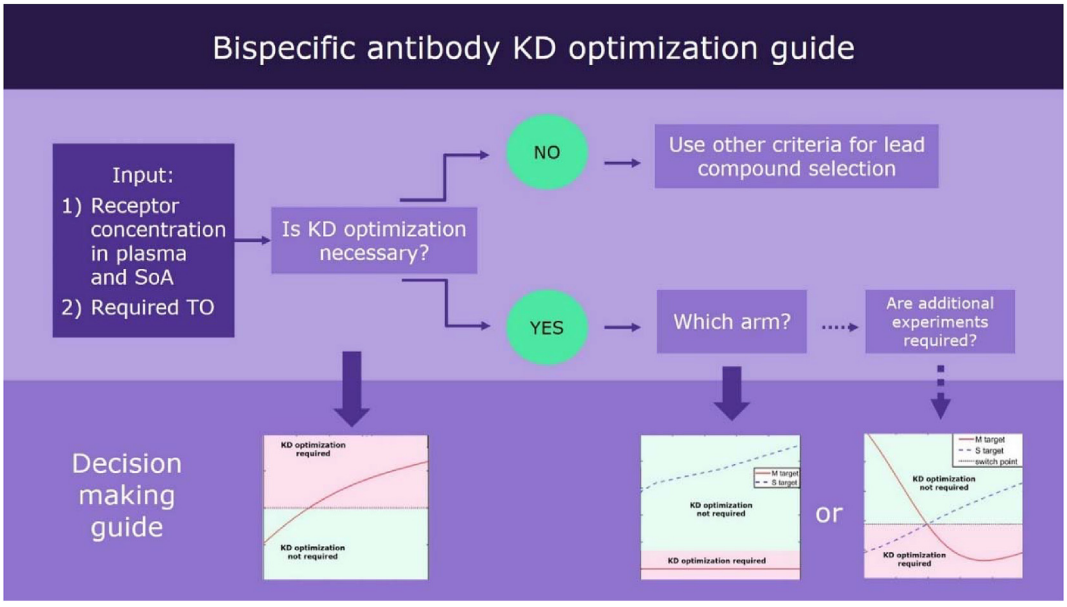

Figure 4. Overview of bispecific antibody KD optimization guide.

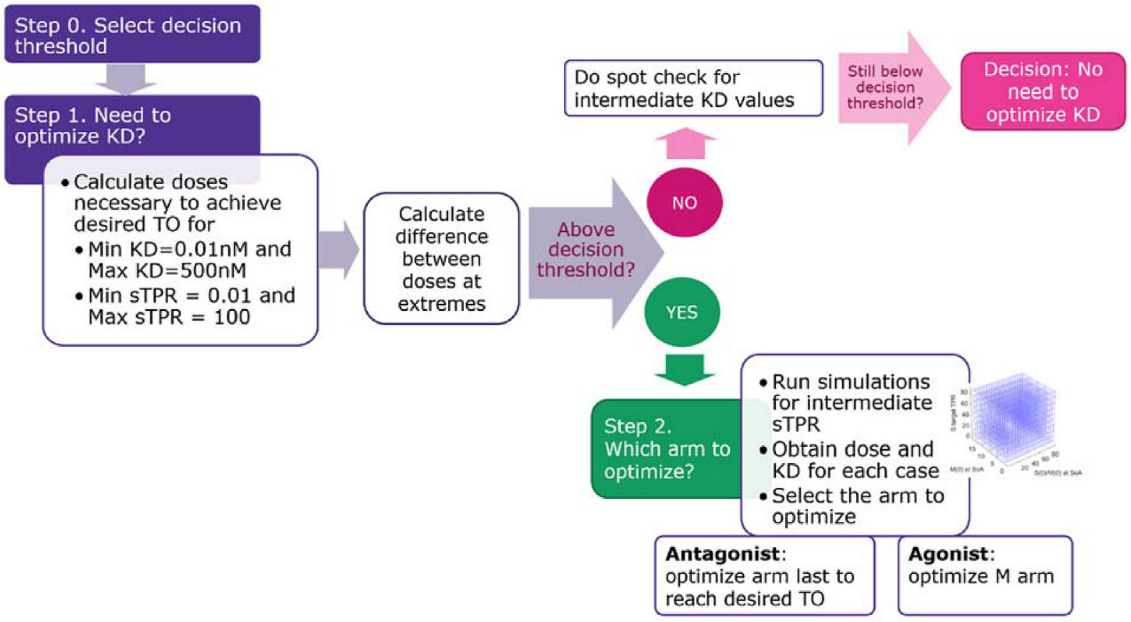

Figure 5. Process summary for KD optimization of bispecific antibodies.

Next, we present examples that showcase the use of this method. Summary of conditions for each case and the corresponding outcomes are given in Table 1. For this set of case studies, we assume that initial concentration of membrane-bound target in the SoA is $M_T(0) = 10$, an assumption that can be relaxed as necessary.

3. Results

Case 1. No need to optimize KD; low KD gives lowest dose.

In the first case, we considered an antagonist with a necessary minimum of 60 % level of target engagement on both arms. These values are chosen arbitrarily to illustrate the different outcomes that can be revealed using this methodology. We took concentration of S target in the SoA to be $S_T(0) < 10$ and determined whether KD needs to be optimized, which arm, and whether any additional information about distribution of the target is necessary to make this decision.

Implementing first step in Figure 5, we calculated the difference in predicted doses for simulated KDs ranging from 0.01 nM to 500 nM for both arms of the molecule. In this case, the resulting difference was always 3.2, regardless of concentration of S target in the plasma (Figure 6); therefore, no additional experiments to calculate concentration of target in other compartments are necessary, since there will be no difference in projected optimal KD or the final dose. This result also suggests that low KD will result in lowest dose. In this case, the "dose differential" is relatively small, and thus investment of additional resources into affinity maturation may be unnecessary.

Case 2. Always optimize the M arm; high KD gives lowest dose.

Here we considered an antagonist that is assumed to require a minimum 30 % target occupancy for both targets. Initial concentrations were the same as the previous cases, with $M_T(0) = 10$ and $S_T(0) < 10$. In this case, the first step revealed that the difference between doses necessary to achieve a minimum of 30 % target engagement on both targets at the

Table 1. Conditions used for case studies. (concentrations are in arbitrary units).

	Case 1	Case 2	Case 3	Case 4
Agonist/ Antagonist	Antagonist	Antagonist	Antagonist	Agonist
Desired target occupancy	Min TO = 60%	Min TO = 30%	Min TO = 60%	Max TO = 30%
Initial concentration of M target in tissue	$M_T(0)=10$	$M_T(0)=10$	$M_T(0)=10$	$M_T(0)=10$
Concentration of S target in SoA	$S_T(0)<10$	$S_T(0)<10$	$S_T(0)=10^3$	$S_T(0)=1$
Conclusion	No need to optimize KD	a. High KD gives lowest dose b. Always optimize M arm	a. Low KD gives lowest dose b. sTPR needs to be measured to select arm to be optimized a. S if sTPR<0.4 b. M if sTPR>0.4 c. For sTPR=0.01, predicted dose is prohibitively high	With the constraint of max TO on S arm, achieving more than 2.5% TO on M arm is impossible regardless of KD or sTPR

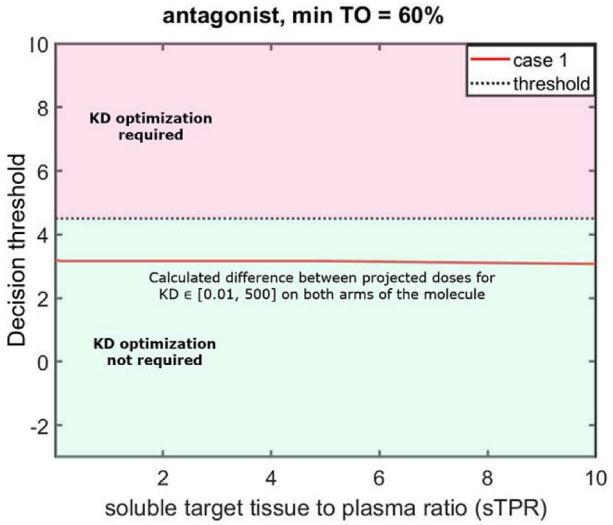

Figure 6. Case 1: no need to optimize KD. According to Step 1 of Figure 5, the difference between predicted doses at selected KD extremes (KD for both targets varied between 0.01 to 500 nM) is the same regardless of concentration of S target in tissue vs plasma compartments; in this case, it is below decision threshold (green region of the figure). Therefore, no additional experiments to calculate S target concentration in different compartments is necessary.

two KD extremes is negative; therefore, it is the high KD that will result in lowest dose (Figure 7A).

Next, we evaluated which arm is the last to reach minimum necessary concentration of 30 % and observed that regardless of other conditions, M arm is always the one to be optimized (Figure 7B).

Case 3. Switch point.

In the third case, we considered an antagonist that is assumed to require a minimum of 60 % level of target engagement on both arms. Concentration of M target was held fixed at $M_T(0) = 10$; however, in this case we assumed that the concentration of S target in the tissue is much larger, with $S_T(0) = 10^3$.

As in the previous cases, we calculated the difference between predicted doses for low and high KD for both arms (Step 1 of Figure 5), and observed that the difference is above the threshold only for some values of sTPR (soluble target tissue to plasma ratio), and therefore, a closer look at specific physiological conditions was warranted to make a decision (Figure 8A). Next (Step 2 of Figure 5), we saw that there exists a "switch point" with respect to sTPR: below sTPR <0.4, S target needs to be optimized but for sTPR >0.4, M target needs to be optimized (Figure 8B). Therefore, additional experiments are required to determine sTPR in order to make the most appropriate decision about KD optimization.

Notably, when sTPR = 0.01, the predicted dose for optimized KD is prohibitively high (in this case 600 mg/kg). For these conditions, a bispecific modality may not be appropriate for targets with these properties.

Case 4. Target combination is unsuitable for a bispecific

Finally, we considered an agonist, where a maximum of 30 % target engagement was assumed to be acceptable; for other parameters, $S_T(0) = 1$, and as in the previous cases, $M_T(0) = 10$. Our analysis showed that regardless of sTPR and KD, by the time S arm reaches maximum acceptable level of target engagement (here 30 %), the maximum TO of the M arm will not exceed 2.4 %. This level of engagement like likely to be pharmacologically ineffective, and therefore for these physiological conditions, a bispecific modality may not be appropriate.

3.1. What makes a target limiting?

As one can see in Case 3, there can exist a "switch point", where one or the other target becomes limiting. We wanted to evaluate conditions that affect when such a "switch point" may occur. For that, we ran numerical experiments for various values of $S_T(0)$, sTPR and desired TO.

In Figure 9, we plotted the conditions under which the "switch point" occurred with respect to sTPR for different levels of desired target occupancy. We ran situations when $M_T(0) = 1$, 10 and 20, and the results were consistent for each case (only results for $M_T(0) = 10$ are shown here), indicating that it is relative rather than absolute target concentrations that impact this value.

More broadly, for antagonists, membrane-bound targets are limiting largely due to higher internalization rates. Soluble targets become limiting when higher TO needs to be achieved, and when the concentration of soluble targets relative to membrane-bound ones is high at the site of action. In these cases, membrane-bound targets "saturate" first. Additionally, since target engagement is calculated as (bound targets)/(bound targets + free targets), large concentrations of the S target relative to M mean that more drug will be necessary to cover it, making S target limiting under these conditions.

Notably, while shed targets were not explicitly covered in the described case studies, the proposed approach can be applied to shed targets as well through model modification. Specifically, to incorporate shed target dynamics, an additional clearance rate, or shedding rate, to a membrane-bound target needs to be introduced, which will serve as the synthesis rate for the soluble shed target; the shed target is then cleared at its own clearance rate, which may be same or different from that of its membrane-bound counterpart, depending on the specific target's biology. The shed target may then distribute into other compartments as

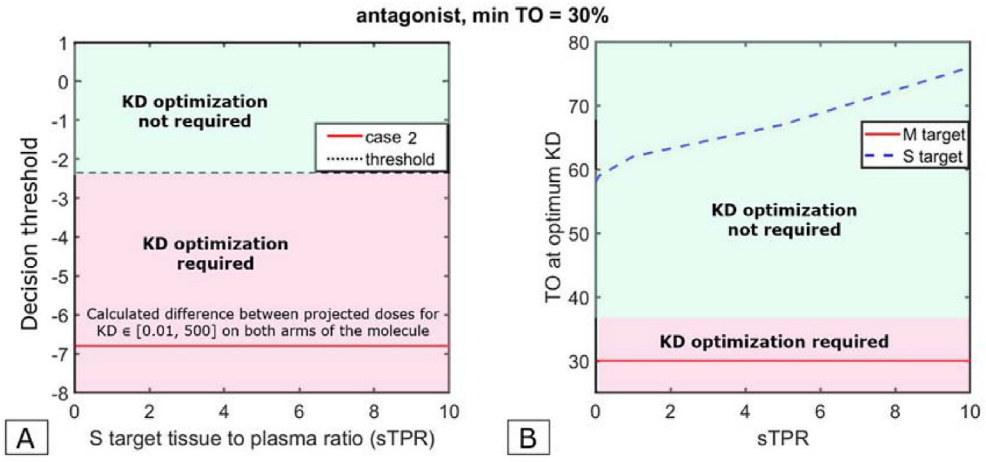

Figure 7. Case 2: always optimize M arm; high KD gives lowest dose. (A) Step 1 of Figure 5 reveals that one of the arms needs to be optimized, and that lowest dose will be achieved with high KD because the calculated difference between projected doses for extreme values of KD is negative and below a decision threshold (red region); threshold is to be chosen based on project-specific considerations. (B) Step 2 of Figure 5 reveals that under these conditions, M arm is always limiting and thus should be optimized; M arm is always last to reach desired TO, so no additional experiments to evaluate tissue to plasma ratio of the S target are necessary.

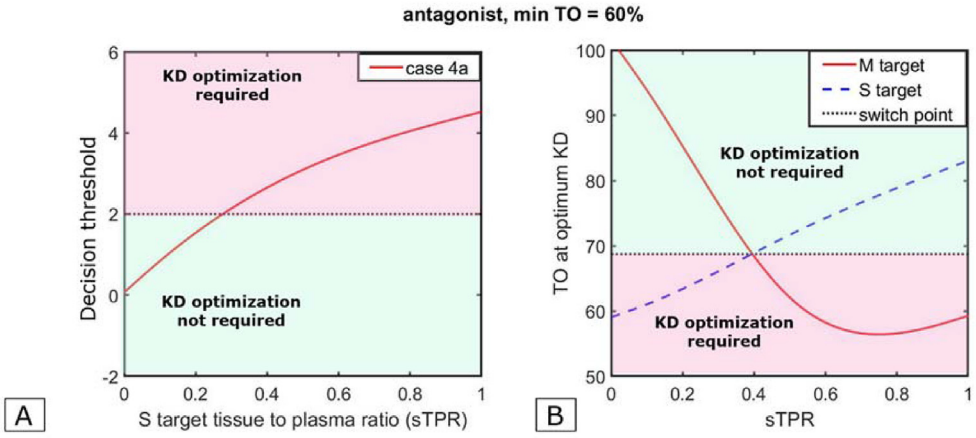

Figure 8. Case 3, antagonist: existence of switch point. (A) Step 1 of Figure 5 suggests that one of the arms needs to be optimized for sTPR <0.3, and that lowest dose will be achieved with low KD on both arms. (B) Step 2 of Figure 5 reveals that for sTPR <0.4, S arm needs to be optimized, while for sTPR >0.4, M arm needs to be optimized. Therefore, additional experiments are required to determine relevant sTPR.

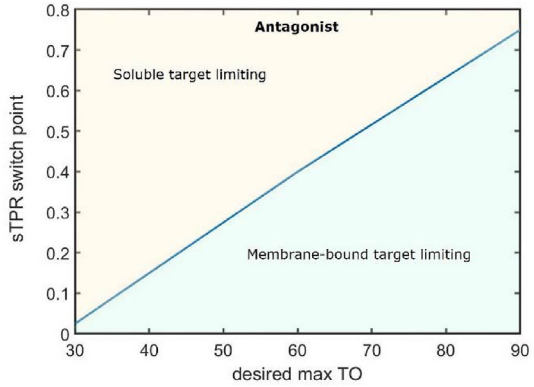

Figure 9. Conditions under which one or the other target become limiting. Here $M_T(0) = 10$; $S_T(0) = 10^3$; results are the same for $M_T(0) = 1$ and 20 (not shown). Other parameters are held constant at values reported in Appendix.

well. While analysis of dynamics of specific cases of shed targets is beyond the scope of this work, with this minor modification to the underlying model equations, the proposed methodology can now be fully applied to shed targets as well.

4. Discussion

Mathematical modeling has become an increasingly important tool for helping advance drug discovery and development into the clinic [15, 16, 17, 18, 19]. While little data is typically available at the earliest stages of drug discovery, it can still be used to help with a logical and meaningful approach to drug candidate selection.

Model-driven lead compound selection process for mono-specifics was presented in [9, 20], highlighting the importance of both KD and intrinsic target properties for decision making. The calculus underlying lead compound selection for bispecifics becomes significantly more complex and non-intuitive, since each target can have different turnover and distribution within the body. Our analysis, started in [11] and continued here, reveals that there are 3 main properties that impact lead compound selection: affinity (KD) of the compound to the target, target turnover and target distribution.

In [11], we looked at target turnover and KD for optimizing lead bispecific compound selection with two membrane-bound targets. Here this analysis was extended to investigate the impact of differences in target distribution throughout the body. We showed that it can significantly impact both the feasibility of engaging two targets using a bispecific modality, and the properties of an optimal compound, defined here as a compound that can achieve a sufficient level of target engagement with the lowest dose. The question of what constitutes a "sufficient level of engagement" warrants further discussion, even at the earliest stages of drug optimization.

4.1. Receptor engagement efficacy model

As was mentioned in the introduction, one of the central assumptions underlying the considered paradigm is the receptor occupancy model, which is based on the premise that receptor engagement can translate to downstream biology and affect disease. Within this paradigm, sufficient receptor engagement is necessary to observe efficacy. In cases when disease is driven by abnormal, often elevated, native signaling, such as in

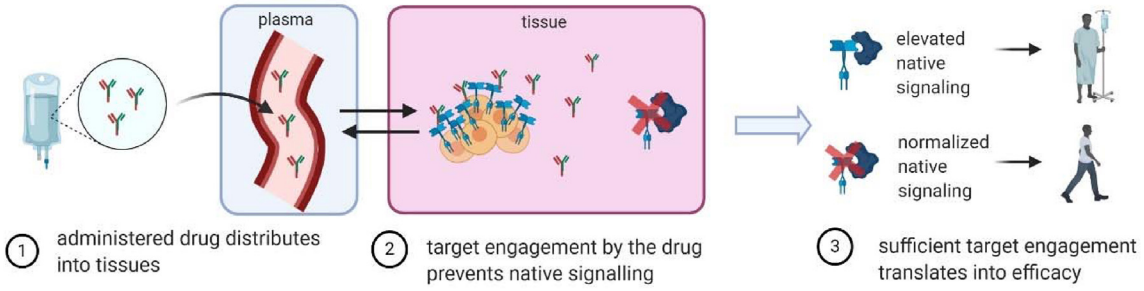

Figure 10. Receptor engagement efficacy model. Underlying assumption of this paradigm is that receptor engagement can normalize native signaling, and thus sufficient target engagement can translate into efficacy.

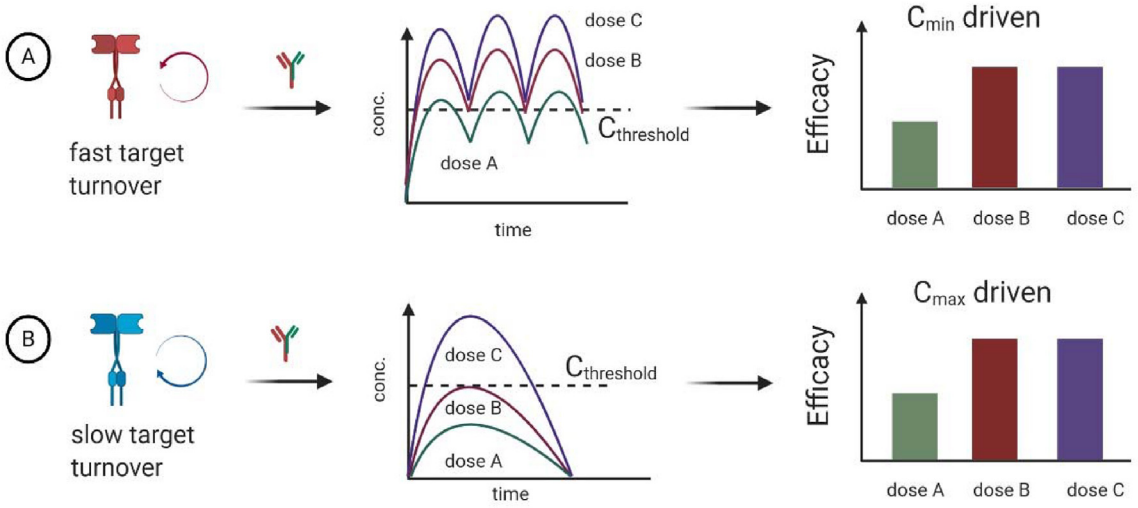

Figure 11. Impact of target turnover on potential dosing strategies. (A) We propose that within the receptor engagement efficacy model, fast target turnover implies need for Cmin driven dosing strategy to maintain a minimum of necessary target coverage above an efficacy threshold.

cancer, sufficient receptor engagement is assumed to result in its normalization (Figure 10).

The extent of receptor engagement necessary to affect disease is a question that warrants discussion. Complete engagement is not always necessary and can potentially result in toxicity, especially for agonists or drugs with suboptimal safety profiles, such as CD3 bispecific constructs [12]. Conversely, insufficient engagement may insufficiently test the underlying biological mechanism, resulting in insufficient proof of pharmacology.

We propose that initial assessments, even at the earliest stages of drug development, can be made from minimal information about target turnover rates. Specifically, we propose that if a target has a fast turnover rate, then in order to effectively interfere with native signaling, continuous engagement may be necessary; this can be interpreted as a "Cmin driven mechanism", where a minimum drug concentration is maintained through a dosing interval, resulting in a minimal level of continuous engagement being necessary for efficacy. This is an approach that is often used for cytotoxic cancer therapies, where continuous target coverage is necessary to interfere with abnormal signaling observed in tumors (example of such drugs include cetuximab, which interferes with EGFR signaling [21], or anti-angiogenesis drugs that interfere with tumor vascularization [22, 23, 24, 25, 26]). For these targets, insufficient engagement can result in underdosing the patient and suboptimal efficacy. With regards to KD optimization, less tight binding might in fact result in higher levels of engagement; this was discussed in more detail in [9, 11].

In contrast, for a target with a slow turnover, once the target is engaged, additional dosing might not translate into additional efficacy. This can be interpreted as a "Cmax driven efficacy". The theoretical predictions for these two cases are summarized in Figure 11.

These considerations are of course not firm guidelines for decision making, and full analysis revealing more precise ranges of "fast" vs "slow" target turnover rates needs to be conducted. Furthermore, there exist additional considerations, such as clock- and counterclockwise hysteresis, which may impact selection of necessary criteria. Nevertheless, they do highlight a need for systematically assessing multiple aspects that go into decision making for lead compound selection, beyond solely drug affinity for its target. With multiple factors at play, mathematical modeling is critical for helping decide whether and what combination of compound and target properties makes it feasible to take a compound to the next stage of drug development, whether for a monospecific or a bispecific compound, and how to maximize success moving forward.

Declarations

Author contribution statement

Irina Kareva: Conceived and designed the experiments; Performed the experiments; Analyzed and interpreted the data; Wrote the paper.

Anup Zutshi: Conceived and designed the experiments; Wrote the paper.

Pawan Gupta: Performed the experiments.

Senthil Kabilan: Conceived and designed the experiments; Performed the experiments.

Funding statement

This work was supported by EMD Serono, a US subsidiary of Merck KGaA.

Data availability statement

Data included in article/supplementary material/referenced in article.

Declaration of interests statement

The authors declare no conflict of interest.

Additional information

No additional information is available for this paper.

Appendix

Model description

The proposed model describes the interactions of a bispecific antibody with a membrane-bound target M(t) and a soluble target S(t). We assume the presence of three distinct compartments in the body: plasma, where the drug is administered, the site-of-action (SoA) compartment, where interactions occur between a BsAb and its targets in a relevant kinetic space, usually considered to be a part of the tissue interstitium (Chudasama et al. 2015), and the peripheral compartment, which represents the other spaces in the body where the drug can distribute.

Notably, SoA models allow for a mathematical representation of the various physicochemical and biochemical processes associated with a drug's distribution, binding to the target and dissociation of the drug-target complex, as well as elimination of the drug and interacting species. SoA models also integrate the physiology of the target in the healthy vs. diseased state. Mathematical details of the SoA models can be found in (Tiwari et al. 2016; Brodfuehrer et al. 2014).

We track the kinetics over time of free drug concentration in the plasma $D_P(t)$, free drug in the peripheral compartment $D_{Ph}(t)$, and free drug at the SoA $D_T(t)$, as well as the dynamics of membrane bound target $M(t)$ and soluble target $S(t)$, and the corresponding drug-target complexes $DM(t)$ and $DS(t)$. Here we assume no distribution of the soluble target into the plasma compartment and hence no kinetic interactions in that compartment; this assumption can be relaxed as necessary.

The drug is assumed to be administered via intravenous bolus. Once distributed in the plasma compartment, free drug $D_P(t)$ can be eliminated at a rate k_{el}, can partition into the SoA at a rate k_{PT}, or partition back from the SoA at a rate $k_{TP}\frac{V_T}{V_P}$, where V_P is the volume of plasma compartment, and V_T is the volume of the SoA compartment. Free drug in plasma can also partition into the peripheral compartment at a rate k_{PPh}, or partition back at a rate $k_{PhP}\frac{V_{Ph}}{V_P}$, where V_{Ph} is the volume of the peripheral compartment. Free drug in the SoA $D_T(t)$ is distributed from the plasma at a rate $k_{PT}\frac{V_P}{V_T}$. Following distribution, free drug $D_T(t)$ can bind to a membrane-bound target $M(t)$ with a second order rate constant k_{on_M} and dissociate with a first order rate constant k_{off_M}, where the affinity of the drug to the target is defined as $K_D = \frac{k_{off}}{k_{on}}$. In a similar sequence the drug $D_T(t)$ in the SoA can also bind to the soluble target $S(t)$ with a second order rate constant k_{on_S} and dissociate with a first order rate constant k_{off_S}.

The dynamics of the membrane drug-target complex $DM(t)$ is determined by previously described association and dissociation rates k_{on_M} and k_{off_M}. The complex can also be internalized at a rate k_{int_M}. Similarly, the soluble drug-target complex $DS(t)$, both in the plasma or in the SoA, is determined by previously described association and dissociation rates k_{on_S} and k_{off_S}, and can be cleared at a rate k_{deg_S}. It is assumed that the complex $DS(t)$ can also transport between plasma compartment and SoA at the same rates as $D_T(t)$.

Finally, target $M(t)$ is synthesized at a zero order rate k_{syn_M}, internalized at a first order rate k_{int_M}, and can bind to either the free drug, or the drug-target complex $DS(t)$ to form the trimeric complex $DSM(t)$. Similarly, the target $S(t)$ is synthesized at a zero order rate k_{syn_S}, cleared at a first order rate k_{deg_S}, and can bind to either the free drug, or the drug-target complex $DM(t)$ to form $DSM(t)$. Furthermore, we assume that the soluble target $S(t)$ can diffuse between plasma and SoA at rates k_{PT_S} and k_{TP_S}, respectively. In the plasma compartment, it can bind to the drug $D_P(t)$ at a rate k_{on_S} and dissociate at a rate k_{off_S}, as in the SoA.

These interactions are captured by the following system of ODEs:

$$\frac{dD_P}{dt} = -k_{el}\cdot D_P - k_{PT}\cdot D_P + \frac{V_T}{V_P}\cdot k_{TP}\cdot D_T - k_{PPh}\cdot D_P + \frac{V_{Ph}}{V_P}\cdot k_{PhP}\cdot D_{Ph} - k_{on_S}\cdot D_P\cdot S_P + k_{off_S}\cdot DS_P$$

$$\frac{dD_{Ph}}{dt} = \frac{V_P}{V_{Ph}}\cdot k_{PPh}\cdot D_P - k_{PhP}\cdot D_{Ph}$$

$$\frac{dD_T}{dt} = \frac{V_P}{V_T}\cdot k_{PT}\cdot D_P - k_{TP}\cdot D_T - k_{on_M}\cdot D_T\cdot M_T + k_{off_M}\cdot DM_T - k_{on_S}\cdot D_T\cdot S_T + k_{off_S}\cdot DS_T$$

$$\frac{dDM_T}{dt} = k_{on_M}\cdot D_T\cdot M_T - k_{off_M}\cdot DM_T - k_{int_M}\cdot DM_T - k_{on_S}\cdot DM_T\cdot S_T + k_{off_S}\cdot DMS_T$$

$$\frac{dDS_T}{dt} = -k_{deg_S}\cdot DS_T + k_{on_S}\cdot D_T\cdot S_T - k_{off_S}\cdot DS_T - k_{on_M}\cdot DS_T\cdot M_T + k_{off_M}\cdot DMS_T - k_{TP}\cdot DS_T + \frac{V_P}{V_T}\cdot k_{PT}\cdot DS_P$$

$$\frac{dDS_P}{dt} = -k_{el}\cdot DS_P + k_{on_S}\cdot D_p\cdot S_P - k_{off_S}\cdot DS_P - k_{PT}\cdot DS_P + \frac{V_T}{V_P}\cdot k_{TP}\cdot DS_T$$

$$\frac{dDMS_T}{dt} = k_{on_S}\cdot DM_T\cdot S_T - k_{off_S}\cdot DMS_T + k_{on_M}\cdot DS_T\cdot M_T - k_{off_M}\cdot DMS_T - k_{int_M}\cdot DMS_T$$

$$\frac{dS_P}{dt} = k_{syn_S} - k_{deg_S}\cdot S_P + \frac{V_T}{V_P}\cdot k_{TP_S}\cdot S_T - k_{PT_S}\cdot S_P - k_{on_S}\cdot D_P\cdot S_P + k_{off_S}\cdot D_PS_P$$

$$\frac{dS_T}{dt} = k_{syn_S} - k_{deg_S}\cdot S_T - k_{on_S}\cdot D_T\cdot S_T + k_{off_S}\cdot DS_T - k_{on_S}\cdot DM_T\cdot S_T + k_{off_S}\cdot DMS_T - k_{TP_S}\cdot S_T + \frac{V_P}{V_T}\cdot k_{PT_S}\cdot S_P$$

$$\frac{dM_T}{dt} = k_{syn_M} - k_{deg_M}\cdot M_T - k_{on_M}\cdot D_T\cdot M_T + k_{off_M}\cdot DM_T - k_{on_M}\cdot DS_T\cdot M_T + k_{off_M}\cdot DMS_T$$

A diagram summarizing these interactions is given in Figure 2 of the main text.

Parameters

Similar to our work in our previous model (Kareva et al. 2018), parameters used in this model can be subdivided into three categories: 1) Physiological compartment parameters, 2) BsAb PK parameters and 3) Target-related parameters.

Physiological parameters include volumes of plasma and SoA compartments V_P and V_T, respectively. They are typically estimated from PK data, as are drug clearance and distribution rates from plasma and SoA compartments, Cl_P and Cl_T respectively. With these values, it is easy to estimate the rate of drug distribution from plasma to SoA to be $k_{PT} = \frac{Cl_T}{V_P}$ and rate of drug distribution from SoA back to plasma to be $k_{TP} = \frac{Cl_T}{V_T}$.

The value of dissociation constant K_D, which is defined as $K_D = \frac{k_{off}}{k_{on}}$, is typically experimentally estimated using Biacore®, or other methods. Foote and Eisen (Foote & Eisen 1995) estimated k_{on} for large molecules to be in the range of $10^5 - 10^6\ M^{-1}s^{-1}$, which will be fixed in the current model, especially when the latter is not measured. This allows estimation of k_{off} from $K_D$values for various interactions.

Finally, target elimination rate can be estimated from its half-life (THL): assuming first order kinetics, $k_{deg} = \frac{ln(2)}{THL}$. Rate of target synthesis can then be calculated from target baseline levels as $k_{syn} = k_{deg}{}^*R_0$, where R_0 is the homeostatic baseline level of the target. It is likely to vary between healthy and disease states, which should be considered for modeling purposes.

A summary of sample parameter values used in our model is given in Table 1. Parameter values were primarily obtained from (Dirks & Meibohm 2010; Le Dirks 2010; Gibiansky & Gibiansky 2009; Gibiansky 2011). Notably, these values will vary depending on the molecule and targets studied.

Supplementary Table 1. Description, units and sample values of parameters used in System [1].

Parameter	Description	Units	Sample value	Ref.
Physiological parameters				
V_P	Volume of plasma compartment	L	3.06	Tiwari et al.
V_{Ph}	Volume of peripheral compartment	L	3.1	Tiwari et al.
V_T	Volume of tissue (SoA) compartment	L	0.192	(Davies & Morris 1993)
BsAb Pharmacokinetics				
Cl_P	Rate of drug clearance from plasma	L/day	1.32	(Gibiansky 2011)
CL_S	Distribution clearance of cytokine (soluble receptor)	L/day	0.504	(Chudasama et al. 2015)
k_{PPh}	Drug transfer rate from peripheral compartment to plasma	1/day	0.186	(Tiwari et al. 2016)
k_{Php}	Drug transfer rate from plasma to peripheral compartment	1/day	0.184	(Tiwari et al. 2016)
k_{TP}	Drug transfer rate from SoA to plasma	1/day	0.186	Assumed same as k_{PPh}
k_{PT}	Drug transfer rate from plasma to SoA	1/day	0.184	Assumed same as k_{PhP}
Target properties				
K_{D_M} / K_{DS}	Equilibrium dissociation constant for drug-target binding. In the simulations, KD for both arms of the molecule is varied from 0.01 to 500 nM. The approach summarized in Figure 5 is then applied to determine whether there is a benefit to optimizing KD at all, and if so, whether there is a particular arm of the molecule that should be the focus of optimization efforts	nM	0.01–500	(Gibiansky 2011)
k_{onM} / k_{onS}	Second order rate constant of drug binding to target	nM/day	1.32	(Foote & Eisen 1995)
$k_{off\,M}$ / $k_{off\,S}$	First order dissociation rate constant of the drug	1/day	$k_{off} = K_D \cdot k_{on}$	calculated
R_{0_M} / R_{0S}	Baseline Concentration of membrane bound and soluble target	nM	0.1	(Gibiansky 2011)
$k_{int\,M}$	Internalization rate for membrane bound target	1/day	50	(Gibiansky 2011)
$k_{int\,S}$ / $k_{deg\,S}$	Degradation/Internalization rate for soluble target	1/day	0.1	(Gibiansky 2011)
k_{PT_S}	Soluble receptor transfer rate from plasma to SoA compartment $(\frac{CL_S}{V_P})$	1/day	0.165	Based on (Chudasama et al. 2015)
k_{TP_S}	Soluble receptor transfer rate from SoA to plasma compartment $k_{PT} = 0.3 \cdot k_{TP} \cdot (\frac{V_T}{V_P})$	1/day	8.75	Based on (Chudasama et al. 2015)

References

[1] D.M. Pardoll, The blockade of immune checkpoints in cancer immunotherapy, Nat. Rev. Cancer 12 (4) (2012) 252–264. Nature Publishing Group.

[2] A.M. Eggermont, M. Maio, C. Robert, Immune checkpoint inhibitors in melanoma provide the cornerstones for curative therapies, Semin. Oncol. (2015) 429–435. Elsevier.

[3] J.W. Kim, J.R. Cochran, Targeting ligand–receptor interactions for development of cancer therapeutics, Curr. Opin. Chem. Biol. 38 (2017) 62–69. Elsevier.

[4] E. Cogollo, M.A. Silva, D. Isenberg, Profile of atacicept and its potential in the treatment of systemic lupus erythematosus, Drug Des. Dev. Ther. 9 (2015) 1331. Dove Press.

[5] B.H. Rovin, R. Furie, K. Latinis, R.J. Looney, F.C. Fervenza, J. Sanchez-Guerrero, et al., Efficacy and safety of rituximab in patients with active proliferative lupus nephritis: the Lupus Nephritis Assessment with Rituximab study, Arthritis Rheum. 64 (4) (2012) 1215–1226. Wiley Online Library.

[6] S.V. Navarra, R.M. Guzmán, A.E. Gallacher, S. Hall, R.A. Levy, R.E. Jimenez, et al., Efficacy and safety of belimumab in patients with active systemic lupus erythematosus: a randomised, placebo-controlled, phase 3 trial, Lancet 377 (9767) (2011) 721–731. Elsevier.

[7] E.F. Morand, R. Furie, Y. Tanaka, I.N. Bruce, A.D. Askanase, C. Richez, et al., Trial of anifrolumab in active systemic lupus erythematosus. New England Journal of Medicine, Mass Med. Soc. 382 (3) (2020) 211–221.

[8] J.E. Peterson, D. Zurakowski, J.E. Italiano Jr., L.V. Michel, S. Connors, M. Oenick, et al., VEGF, PF4 and PDGF are elevated in platelets of colorectal cancer patients, Angiogenesis 15 (2) (2012) 265–273. Springer.

[9] A. Tiwari, A.K. Abraham, J.M. Harrold, A. Zutshi, P. Singh, Optimal affinity of a monoclonal antibody: guiding principles using mechanistic modeling, AAPS J. 19 (2) (2017) 510–519. Springer.

[10] V.L. Chudasama, A. Zutshi, P. Singh, A.K. Abraham, D.E. Mager, J.M. Harrold, Simulations of site-specific target-mediated pharmacokinetic models for guiding the development of bispecific antibodies, J. Pharmacokinet. Pharmacodyn. 42 (1) (2015) 1–18. Springer.

[11] I. Kareva, A. Zutshi, S. Kabilan, Guiding principles for mechanistic modeling of bispecific antibodies, Prog. Biophys. Mol. Biol. 139 (2018) 59–72. Elsevier.
[12] H. Saber, P. Del Valle, T.K. Ricks, J.K. Leighton, An FDA oncology analysis of CD3 bispecific constructs and first-in-human dose selection, Regul. Toxicol. Pharmacol. 90 (2017) 144–152. Elsevier.
[13] S.L. Maude, D. Barrett, D.T. Teachey, S.A. Grupp, Managing cytokine release syndrome associated with novel T cell-engaging therapies, Cancer J. 20 (2) (2014) 119. NIH Pub. Access.
[14] J.D. Urban, W.P. Clarke, M. Von Zastrow, D.E. Nichols, B. Kobilka, H. Weinstein, et al., Functional selectivity and classical concepts of quantitative pharmacology, J. Pharmacol. Exp. Therapeut. 320 (1) (2007) 1–13.
[15] M.E. Spilker, P. Singh, P. Vicini, Mathematical modeling of receptor occupancy data: a valuable technology for biotherapeutic drug development, Cytometry B Clin. Cytometry 90 (2) (2016) 230–236. Wiley Online Library.
[16] O.E. Della Pasqua, PKPD and Disease Modeling: Concepts and Applications to Oncology, Clin. Trial Simulat. (2011) 281–306. Springer.
[17] G. Helmlinger, V. Sokolov, K. Peskov, K.M. Hallow, Y. Kosinsky, V. Voronova, et al., Quantitative systems pharmacology: an exemplar model building workflow with applications in cardiovascular, Metabolic and oncology drug development, CPT Pharmacometrics Syst. Pharmacol. (2019). Wiley Online Library.
[18] V. Chelliah, G. Lazarou, S. Bhatnagar, J.P. Gibbs, M. Nijsen, A. Ray, et al., Quantitative Systems Pharmacology approaches for Immuno-oncology: adding virtual patients to the development paradigm, Clin. Pharmacol. Therapeut. (2020). Wiley Online Library.
[19] A.P. Singh, Y.G. Shin, D.K. Shah, Application of pharmacokinetic-pharmacodynamic modeling and simulation for antibody-drug conjugate development, Pharmaceut. Res. 32 (11) (2015) 3508–3525. Springer.
[20] A. Tiwari, H. Luo, X. Chen, P. Singh, I. Bhattacharya, P. Jasper, et al., Assessing the impact of tissue target concentration data on uncertainty in in vivo target coverage predictions, CPT Pharmacometrics Syst. Pharmacol. 5 (10) (2016) 565–574. Wiley Online Library.
[21] J. Kurai, H. Chikumi, K. Hashimoto, K. Yamaguchi, A. Yamasaki, T. Sako, et al., Antibody-dependent cellular cytotoxicity mediated by cetuximab against lung cancer cell lines, Clin. Cancer Res. 13 (5) (2007) 1552–1561.
[22] G.N. Naumov, E. Bender, D. Zurakowski, S.-Y. Kang, D. Sampson, E. Flynn, et al., A model of human tumor dormancy: an angiogenic switch from the nonangiogenic phenotype, J. Natl. Cancer Inst. 98 (5) (2006) 316–325. Oxford University Press.
[23] C. Chen, S. Parangi, M.J. Tolentino, J. Folkman, A strategy to discover circulating angiogenesis inhibitors generated by human tumors. Cancer research, AACR 55 (19) (1995) 4230–4233.
[24] J. Folkman, Angiogenesis: an organizing principle for drug discovery? Nat. Rev. Drug Discov. 6 (4) (2007) 273–286. Nature Publishing Group.
[25] J. Folkman, Role of angiogenesis in tumor growth and metastasis, Semin. Oncol. (2002) 15–18. Elsevier.
[26] R.K. Jain, Normalizing tumor vasculature with anti-angiogenic therapy: a new paradigm for combination therapy, Nat. Med. 7 (9) (2001) 987. Nature Publishing Group.